Electronic Supplementary Information

Enhancing Photovoltaic Performance of Heteroheptacene-Based Nonfullerene Acceptors through Synergistic Effect of Side-Chain Engineering and Fluorination

Dongdong Cai,[a] Jianqi Zhang,[b] Jinyun Wang,[a] Yunlong Ma,[a] Shuo Wan,[ac] Pengsong Wang,[ac] Zhixiang Wei,*[b] and Qingdong Zheng*[a]

[a]State Key Laboratory of Structural Chemistry, Fujian Institute of Research on the Structure of Matter, Chinese Academy of Sciences, 155 Yangqiao West Road, Fuzhou 350002, China. E-mail: qingdongzheng@fjirsm.ac.cn

[b]Key Laboratory of Nanosystem and Hierarchical Fabrication, National Center for Nanoscience and Technology, Beijing 100190, China. E-mail: weizx@nanoctr.cn

[c]University of Chinese Academy of Sciences, 19 Yuquan Road, Beijing 100049, China.

Reagents and instruments

Unless stated otherwise, all chemical reagents were purchased from Aldrich Inc., Adamas-beta Ltd. and Energy Chemical and used directly without additional purification. Chloroform and pyridine were dried with 4Å molecular sieves for reactions. All chemical reactions were performed under an inert atmosphere of nitrogen. High-resolution mass spectroscopy (HRMS) measurements were determined on a Thermo Scientific QExactive mass spectrometer. ^{1}H NMR (^{13}C NMR) spectra were recorded at 400 MHz (100 MHz) on a Bruker AVANCE-400 spectrometer using tetramethylsilane (TMS) as the internal standard. Elemental analyses were carried out by using a Vario EL-Cube elemental analyzer. Absorption spectra were collected from a Lambda 365 UV-vis spectrophotometer. Photoluminescence spectra were collected on a Cary spectrophotometer. Cyclic voltammetry (CV) measurement was performed on a CHI 604E electrochemical workstation with a three-electrode cell in a nitrogen bubbled tetrabutylammonium hexafluorophosphate (Bu_4NPF_6) solution (0.1 M in acetonitrile) at a scan rate of 100 mV s^{-1} at room temperature. Platinum wire, Ag/AgNO$_3$ (0.1 M of AgNO$_3$ in acetonitrile) and platinum plate were used as the counter electrode, reference electrode and working electrode, respectively. The

Ag/AgNO$_3$ reference electrode was calibrated using a ferrocene/ferrocenium redox couple as an external standard, whose oxidation potential is set at -4.80 eV with respect to the vacuum level. The acceptor films were coated on the Pt plate electrode by dipping the electrode into the corresponding acceptor material solutions and then drying. The HOMO energy level was calculated from the equation of $E_{HOMO} = -(\varphi_{ox} + 4.82)$ (eV). The LUMO level was obtained from the equation of $E_{LUMO} = -(\varphi_{red} + 4.82)$ (eV). Surface morphology images were obtained using AFM at a tapping mode.

Synthesis of nonfullerene acceptors

Synthesis of M1. Compound **1a** (100 mg, 0.109 mmol) and 2-(3-oxo-2,3-dihydroinden-1-ylidene)malononitrile (169 mg, 0.873 mmol) were dissolved in dry chloroform (20 mL). After the solution was bubbled with N$_2$ for 30 min, dry pyridine (0.1 mL) was syringed into the solution in one portion. Then, the mixture was stirred at 60 ^{o}C for 6 h. After cooling down to room temperature, the mixture was concentrated with rotary evaporation in vacuum to obtain the crude product, which was quickly purified through column chromatography using petroleum ether/dichloromethane (2:1, *v/v*) as eluent to obtain M1 as a dark blue solid (109 mg, 86%). ^{1}H NMR (CDCl$_3$, 400 MHz, ppm): 8.99 (s, 2H), 8.70 (d, J = 6.0 Hz, 2H), 7.93 (dd, J_1 = 7.7 Hz, J_2 =5.9 Hz, 4H), 7.76 (m, 4H), 4.78 (t, J = 12.0 Hz, 4H), 4.05 (m, 4H), 2.09 (m, 2H), 1.96 (m, 2H), 1.73-1.42 (m, 16H), 1.14-0.97 (m, 28H), 0.79-0.73 (m, 12H); ^{13}C NMR (100 MHz, CDCl$_3$, ppm): 188.3, 160.9, 147.8, 144.8, 140.0, 138.9, 137.3, 136.8, 134.9, 134.3, 131.9, 126.6, 125.2, 123.7, 121.6, 120.0, 116.9, 115.2, 115.1, 79.0, 67.9, 52.7, 40.5, 40.3, 30.2, 29.7, 29.1, 27.9, 23.5, 23.3, 23.1, 22.9, 14.2, 13.8, 11.2, 10.5, 10.4; HRMS (MALDI) m/z: calc. for C$_{76}$H$_{80}$N$_6$O$_4$S$_4$: 1269.5123; found: 1269.5159; Elemental Analysis (%) calc. for C$_{76}$H$_{80}$N$_6$O$_4$S$_4$: C, 71.89; H, 6.35; N, 6.62; found: C, 71.88; H, 6.36; N, 6.53.

Synthesis of M4. M4 was prepared according to the same procedure as that for M1 except for the change of the reaction temperature from 60 ^{o}C to 50 ^{o}C. Compound **1b** (100 mg, 0.097 mmol) and 2-(5,6-difluoro-3-oxo-2,3-dihydro-1H-inden-1 -

ylidene)malononitrile (179 mg, 0.777 mmol) were used for the reaction. Finally, a dark blue solid (M4) was obtained (101 mg, 82%). ^{1}H NMR (CDCl$_3$, 400 MHz, ppm): 8.95 (s, 2H), 8.50 (m, 2H), 7.90 (s, 2H), 7.69 (t, J = 7.2 Hz, 2H), 4.78 (d, J = 6.4 Hz, 4H), 4.06 (d, J = 6.0 Hz, 4H), 2.13 (m, 2H), 1.95 (m, 2H), 1.68 (m, 4H), 1.41-0.91 (m, 56H), 0.81-0.71 (m, 12H); ^{13}C NMR (100 MHz, CDCl$_3$, ppm): 185.9, 158.6, 155.7, 154.9, 152.9, 147.9, 145.3, 144.9, 138.9, 137.2, 137.0, 136.6, 136.5, 134.5, 134.4, 132.6, 132.6, 127.0, 120.6, 120.2, 117.1, 114.9, 114.7, 114.6, 112.6, 112.4, 79.6, 68.3, 52.7, 40.3, 39.2, 31.9, 31.2, 30.8, 29.2, 27.9, 27.0, 23.3, 23.3, 23.2, 23.1, 22.9, 22.7, 14.2, 13.8, 10.5, 10.4; HRMS (MALDI) m/z: calc. for C$_{84}$H$_{92}$F$_4$N$_6$O$_4$S$_4$: 1452.5999; found: 1452.5986; Elemental Analysis (%) calc. for C$_{84}$H$_{92}$F$_4$N$_6$O$_4$S$_4$: C, 69.39; H, 6.38; N, 5.78; found: C, 69.24; H, 6.35; N, 5.69.

Fabrication of polymer solar cells

Polymer solar cells were fabricated with a configuration of ITO/PEDOT:PSS/Active layer/PDIN/Ag. The ITO-coated glass substrates were cleaned in an ultrasonic bath with detergent, water, acetone, and isopropyl alcohol for 15 min each and then dried in an oven at 80 ^{o}C for 12 h in the air. After a 20 min UV-O$_3$ zone treatment, a thin layer of PEDOT:PSS (~30 nm) was spin-coated onto the ITO anode and then dried at 140 °C for 15 min. The donor (PM6) and acceptors (M1 and M4) were dissolved in anhydrous chloroform with a concentration of 8 mg/mL for polymer. The solution was stirred at 50 ^{o}C for 5 hours and spin-coated on the PEDOT:PSS-coated ITO glass substrates. The thickness of the active layer was ~130 nm. Then, a thin layer of PDIN was spin-coated onto the active layer at 3000 rpm for 30 s from the methanol solution (2.0 mg/mL). Finally, 100 nm Ag layer was successively thermally evaporated onto the active layer at a pressure of 2.0 × 10^{-4} Pa. The current density-voltage (J-V) characteristics were recorded with a Keithley 2440 source measurement unit under AM 1.5G illumination (100 mW/cm^2) from a Newport solar simulator. A standard silicon solar cell was used to calibrate the light intensity. The external quantum efficiencies (EQE) of the PSCs were measured using a certified Newport incident photon conversion efficiency (IPCE) measurement system.

Hole- and electron-only device fabrication and characterization

Hole and electron mobilities were measured using the space charge limited current (SCLC) method. Hole-only devices were fabricated with an architecture of ITO/PEDOT:PSS/active layer/MoO$_3$/Ag, while electron-only devices were constructed with an architecture of ITO/ZnO/active layer/Ca/Al. The active layers were prepared using the same method as that used for the fabrication of the best-performance polymer solar cells. Device areas were fixed at 4 mm^2. The current-voltage (*J-V*) curves in dark were measured by a Keithley 2440 source measurement unit. The SCLC hole and electron mobilities were calculated according to the following equation:

$$J = \frac{9\varepsilon_0\varepsilon_r\mu V^2}{8L^3}$$

Where *J* is the current density (A m^{-2}), ε_0 is the free-space permittivity (8.85 × 10^{-12} F m^{-1}), ε_r is the relative dielectric constant of the active layer material usually 2-4 for organic semiconductors, herein we used a relative dielectric constant of 3, μ is the hole- or electron-mobility, *V* is the voltage drop across the SCLC electrodes (*V* = *V*$_{app}$-*V*$_{bi}$, where *V*$_{app}$ is the applied voltage to the device, and *V*$_{bi}$ is the built-in voltage due to the difference in the work function of two electrodes for the hole- and electron-only devices, the *V*$_{bi}$ values are 0.5 V and 0.7 V, respectively), and *L* is the thickness of the active layer. The thickness of the film was determined by a Bruker Dektak XT surface profilometer.

GIWAXS characterization

All samples for GIWAXS measurement were prepared on the PEDOT:PSS-coated Si substrates. The 2D GIWAXS patterns were acquired using a XEUSS SAXS/WAXS system at the National Center for Nanoscience and Technology (NCNST, Beijing). The wavelength of the X-ray beam is 1.54 Å, and the incident angle was set as 0.2˚. Scattered X-rays were detected by using a Dectris Pilatus 300 K photon counting detector.

Table S1. Parameters of the ordered structures

Samples[a]	π-π stacking		Lamellar stacking	
	d-spacing (Å)	CL (Å) (FWHM)[b]	d-spacing (Å)	CL (Å) (FWHM)[b]
M1	3.61	9.34 (0.605 Å^{-1})	17.84	39.52 (0.143 Å^{-1})
M4	3.48	26.79 (0.211 Å^{-1})	19.50	62.11 (0.091 Å^{-1})
PM6:M1	3.69	12.17 (0.464 Å^{-1})	21.18	62.89 (0.084 Å^{-1})
PM6:M4	3.58	15.36 (0.368 Å^{-1})	20.34	62.83 (0.053 Å^{-1})
PM6	3.71	10.56 (0.535 Å^{-1})	21.58	62.83 (0.090 Å^{-1})

[a] (010) diffraction peak along the q_z axis, (100) diffraction peak along the q_{xy} axis; [b] Coherent length (CL) estimated from the Scherrer equation (CL = $2\pi K$/FWHM, K = 0.9).

Table S2. Photovoltaic properties of PSCs based on PM6:M4 with different annealing temperatures[a]

Temperature (℃)	V_{OC} [V]	J_{SC} [mA/cm^2]	FF [%]	PCE [%]
80	0.86	22.50	68.0	13.13 (12.79 ± 0.24)[b]
90	0.88	23.49	71.5	14.75 (14.30 ± 0.23)[c]
100	0.85	22.76	68.8	13.27 (12.80 ± 0.32)[b]

[a]The PM6:M4 blends (1:1 by weight) were dissolved in chloroform with 0.5 vol % CN. [b]The average PCEs with standard deviations in parentheses are based on 8 devices. [c]The average PCEs with standard deviations in parentheses are based on 20 devices.

Table S3. Photovoltaic properties of PM6:M4-based PSCs with different blend ratios[a]

D:A (by weight)	V_{oc} [V]	J_{sc} [mA/cm^2]	FF [%]	PCE [%]
1:0.8	0.86	21.81	67.4	12.69 (12.35 ± 0.32)[b]
1:1	0.88	23.49	71.5	14.75 (14.30 ± 0.23)[c]
1:1.2	0.84	22.23	65.9	12.35 (12.03 ± 0.33)[b]

[a]The PM6:M4 blends were dissolved in chloroform with 0.5 vol % CN, and the active layers were annealed at 90 ℃ for 5 min. [b]The average PCEs with standard

deviations in parentheses are based on 8 devices. [c]The average PCEs with standard deviations in parentheses are based on 20 devices.

Table S4. Photovoltaic properties of PM6:M4-based PSCs with different amounts of CN additive[a]

CN (vol %)	V_{oc} [V]	J_{sc} [mA/cm^2]	FF [%]	PCE [%]
0	0.89	22.33	64.0	12.67 (12.24 ± 0.26)[b]
0.5	0.88	23.49	71.5	14.75 (14.30 ± 0.23)[c]
1.0	0.84	20.96	65.2	11.48 (11.18 ± 0.28)[b]

[a]The PM6:M4 blends (1:1 by weight) were dissolved in chloroform, and the active layers were annealed at 90 ^{o}C for 5 min. [b]The average PCEs with standard deviations in parentheses are based on 8 devices. [c]The average PCEs standard deviations in parentheses are based on 20 devices.

Table S5. Photovoltaic properties of PBDB-T:M1-based PSCs[a]

Active layer	V_{oc} [V]	J_{sc} [mA/cm^2]	FF [%]	PCE [%][b]
PBDB-T: M1	0.92	18.56	59.30	10.17 (9.82 ± 0.19)

[a]PBDB-T:M1-based device was prepared according to the same procedure as that for the best-performance PM6:M1-based device. [b]The average PCE with a standard deviation in parentheses is based on 8 devices.
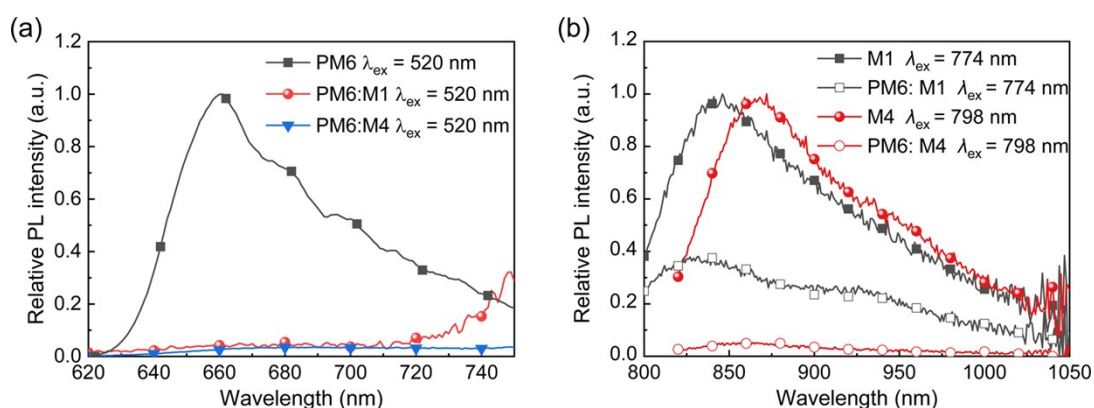

Fig. S1. (a) PL spectra of PM6 neat film, PM6:M1 and PM6:M4 blend films upon an excitation at 520 nm; (b) PL spectra of M1 neat film and PM6:M1 blend film upon an excitation at 774 nm, and PL spectra of M4 neat film and PM6:M4 blend film upon an excitation at 798 nm.
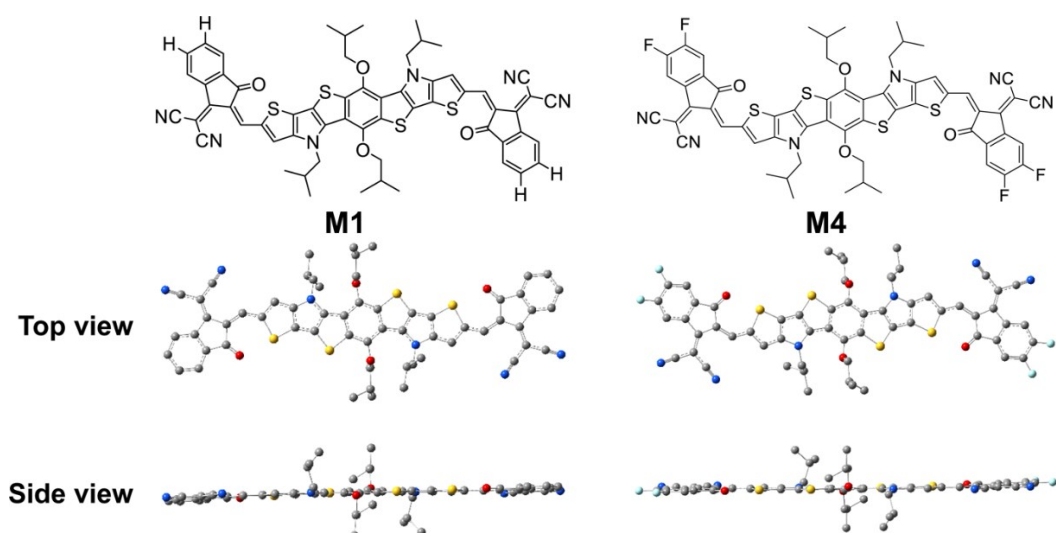
Fig. S2. The optimized geometries for M1 and M4. To simplify the calculations, long branched side chains are replaced by shorter branched ones, and for clarity, hydrogen atoms are not displayed.
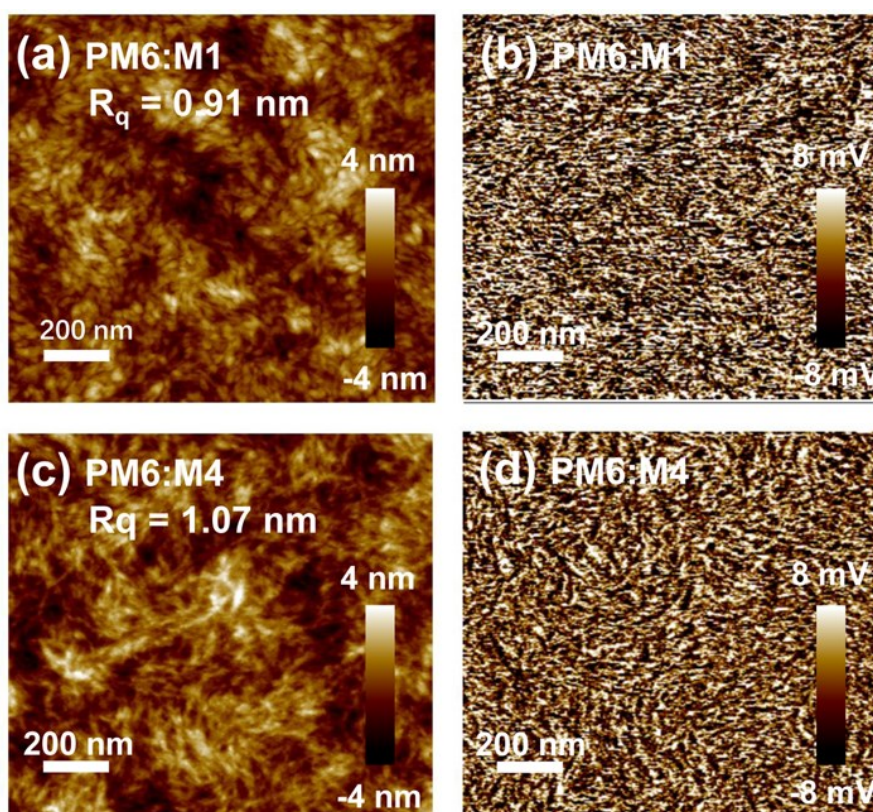

Fig. S3. Tapping mode AFM height (a, c) and phase (b, d) images of the blend films based on PM6:M1 and PM6:M4.